

## Supporting Information

# Electrochemically synthesized polyacrylamide gel and core-shell nanoparticles for 3D cell culture formation

*Nabila Yasmeen,<sup>a</sup> Aneta Karpinska,<sup>a</sup> Jakub Kalecki,<sup>a</sup> Włodzimierz Kutner,<sup>a,b</sup>*

*Karina Kwapiszewska,<sup>a,\*</sup> and Piyush Sindhu Sharma<sup>a,\*</sup>*

<sup>a</sup>Institute of Physical Chemistry, Polish Academy of Sciences, Kasprzaka 44/52, 01-224  
Warsaw, Poland

<sup>b</sup>Faculty of Mathematics and Natural Sciences. School of Sciences, Cardinal Stefan  
Wyszynski University in Warsaw, Wóycickiego 1/3, 01-938 Warsaw, Poland

## **Corresponding Authors**

\*E-mail: psharma@ichf.edu.pl (Piyush Sindhu Sharma)

\*E-mail: kkwapiszewska@ichf.edu.pl (Karina Kwapiszewska)

### **S1. Effect of initiator concentration**

A sufficient amount of peroxydisulfate initiator ions in the aqueous solution for polymerization is necessary to generate a sufficiently high number of active centers that could propagate to undergo a phase transition to form precursor particles or short oligomer chains. Monomers polymerized on these nuclei centers forming soft colloidal gel particles. Therefore, the amount of initiator in the solution was varied. A sufficient number of free radicals was generated in the solution for gel particle preparation at the initiator concentration as low as 15 mM.

### **S2. Effect of polymerization quencher**

This radical polymerization might not be sufficiently quenched after seizing the electrochemical reaction. Therefore, a polymerization inhibitor, vis., hydroquinone monomethyl ether, was added after stopping electroinitiation. Three different inhibitor concentrations were used, i.e., 5, 15, and 25 mM, to study the polymerization chain inhibition effect on the gel particles' morphology (Figure S3). Nevertheless, globular gel particles of different sizes were obtained in each case.

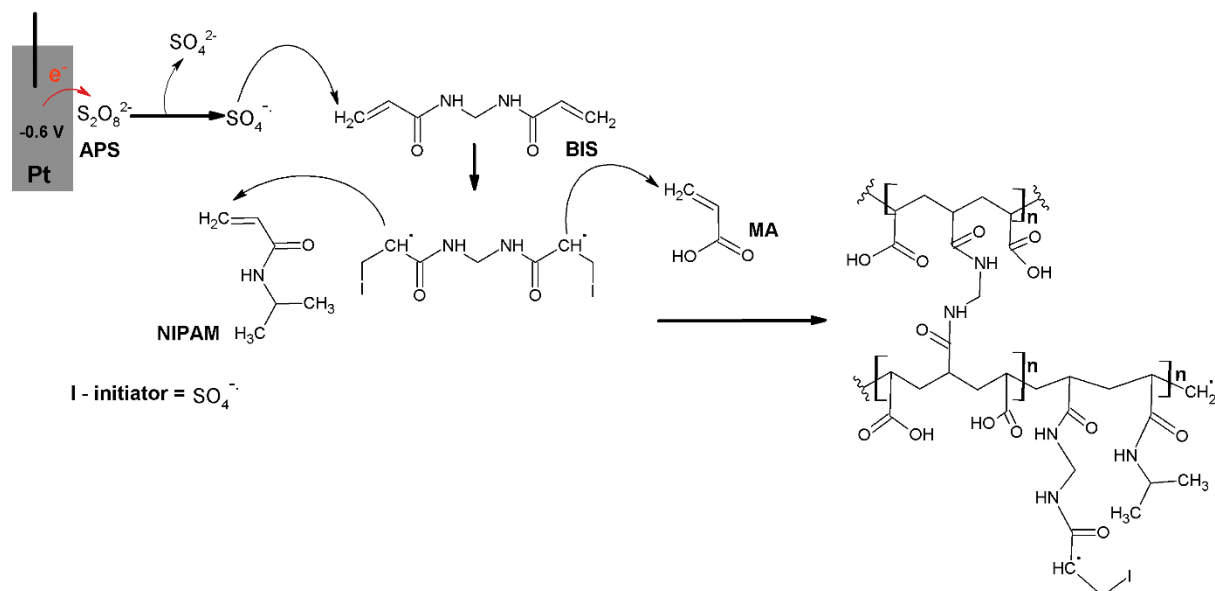
### **S3. The process in the vicinity of the electrode surface**

Electrochemically initiated *N*-isopropylacrylamide, methacrylic acid, and *N,N'*-methylenebisacrylamide polymerization is started by dissociating persulfate at the suitable potential. A pathway of persulfate reduction is proposed below. This pathway involves a direct electron transfer to the anion in the solution.



Similarly, as previously described,<sup>1,2</sup> with time, more and more ammonium persulfate is cleaved at the potential of -0.60 V (Equation S1a), and the amount of water-soluble free radicals becomes sufficient for initiating the polymerization. Kinetic studies of *N,N'*-methylenebisacrylamide and *N*-isopropyl acrylamide copolymerization indicated that the *N,N'*-methylenebisacrylamide monomer reacts faster than the hydrophilic *N*-isopropyl acrylamide monomer (Scheme S1). So in the first step, water-soluble free radicals attack the *N,N'*-methylenebisacrylamide monomer. The *N,N'*-methylenebisacrylamide redox-active center

later targets the *N*-isopropyl acrylamide and methacrylic acid monomer double bonds, resulting in more extended oligomers. Ultimately, these oligomers combine and nucleate to form gel particles.



**Scheme S1.** The tentative mechanism of electrochemically synthesized gel nanoparticles.<sup>1,2</sup>

**BIS** - *N,N'*-methylenebisacrylamide, **MA** - methacrylic acid, and **NIPAM** - *N*-isopropyl acrylamide.

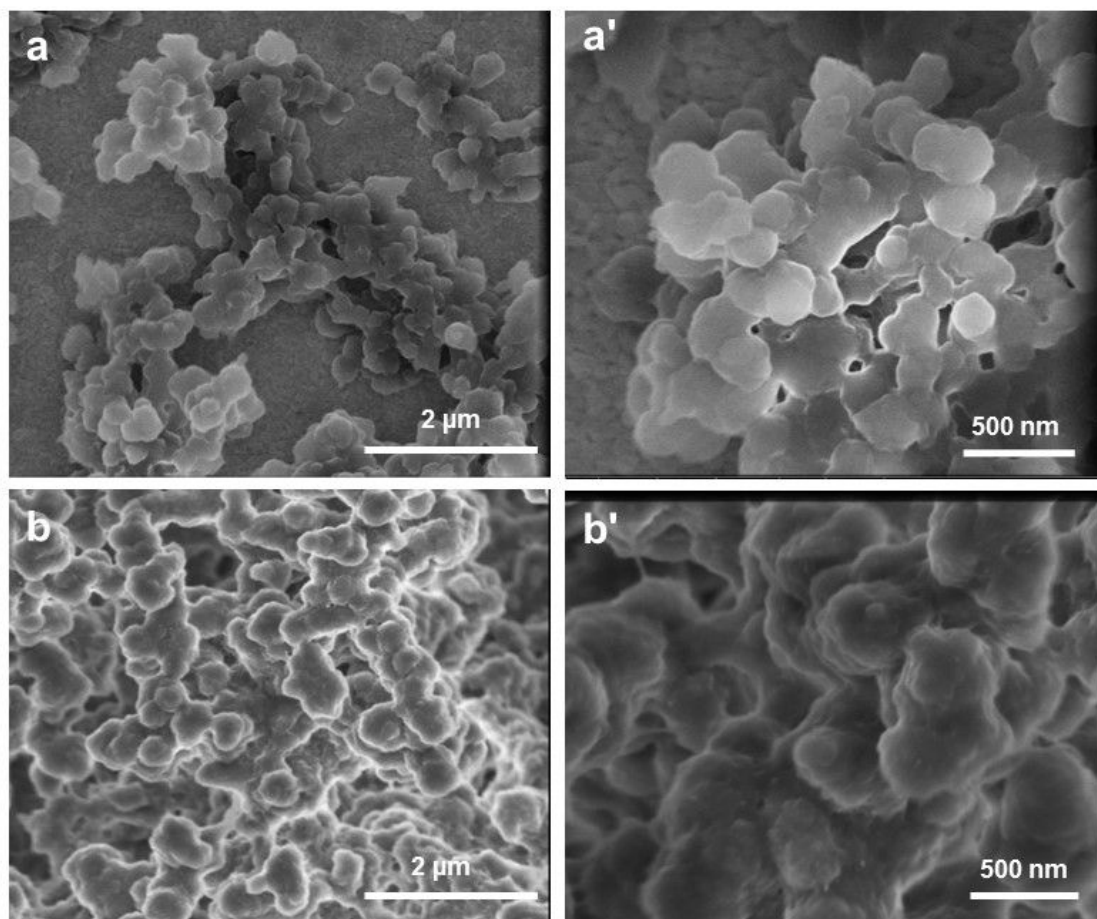


**Figure S1.** The SEM images of **NIPAM-MA-BIS** gels synthesized at the electroinitiation potential of (a, a') -0.70, and (b, b') -0.80 V vs. Ag quasi-reference electrode. The concentrations of **NIPAM**, **MA**, and **BIS** monomers in the solution for polymerization were 25, 25, and 50 mM, respectively.

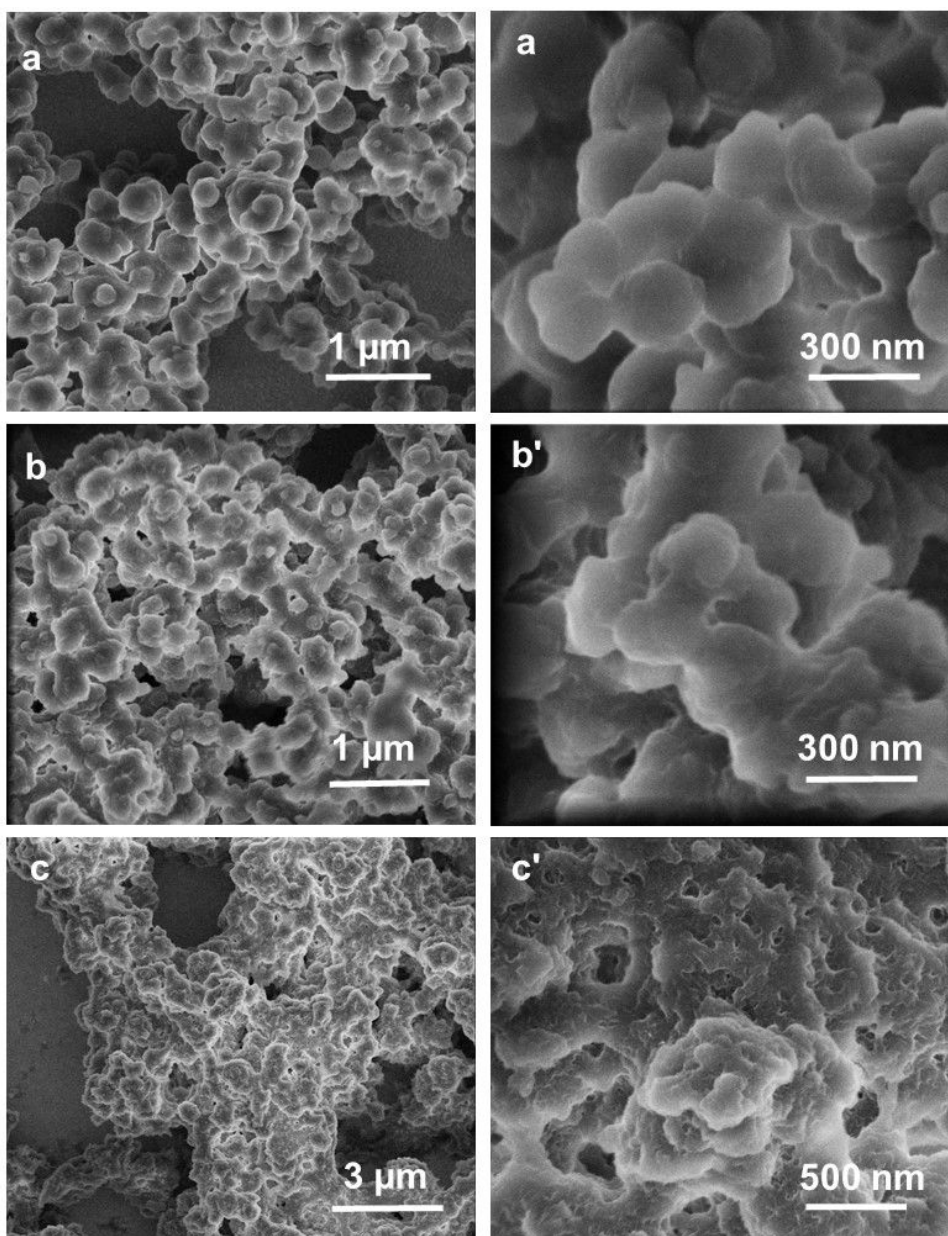


**Figure S2.** The NIPAM-MA-BIS gels' SEM images at the **BIS** cross-linking monomer concentration of (a, a') 5, (b, b') 50, and (c, c') 100 mM. Concentrations of the **NIPAM** and **MA** monomers in the solution for polymerization were 25 mM each.

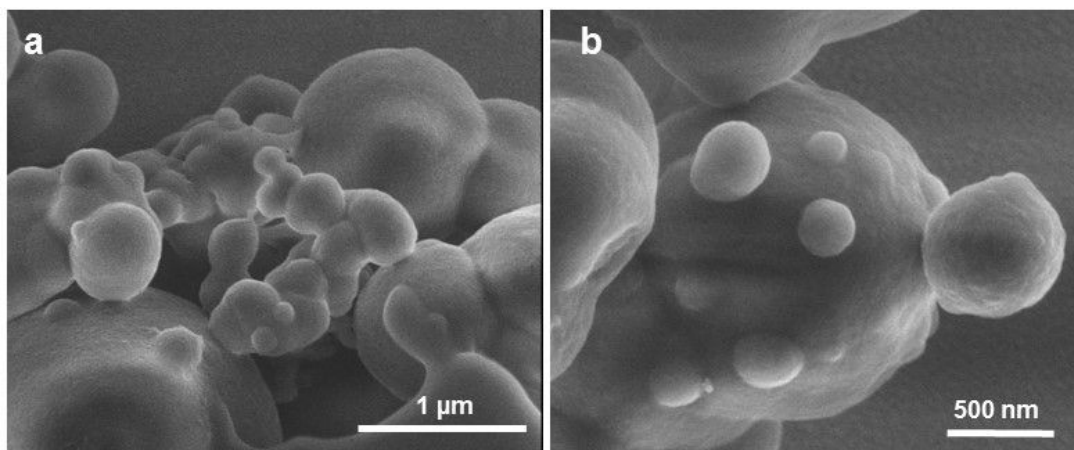


**Figure S3.** SEM images of gel particles prepared after inhibiting polymerization with 15 mM hydroquinone monomethyl ether. The gel was prepared by copolymerizing the **NIPAM**, **MA**, and **BIS** monomer at a 25, 25, and 50 mM concentration.

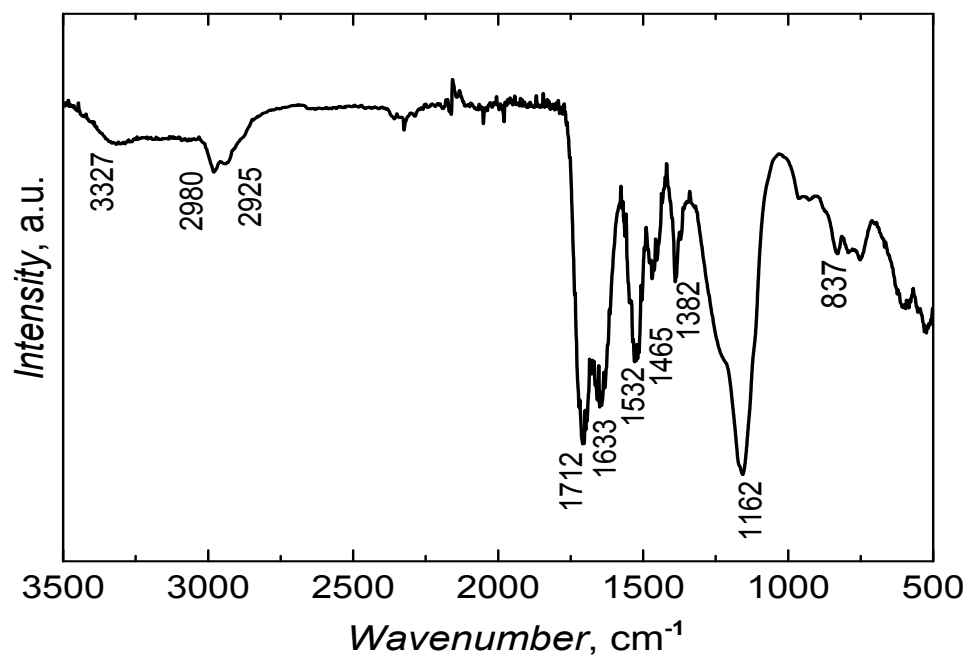


**Figure S4.** The FTIR transmission spectrum of the **NIPAM-MA-BIS** gel prepared by electrochemically initiated copolymerization of the **NIPAM**, **MA**, and **BIS** monomers of the concentration of 20, 20, and 10 mM, respectively.



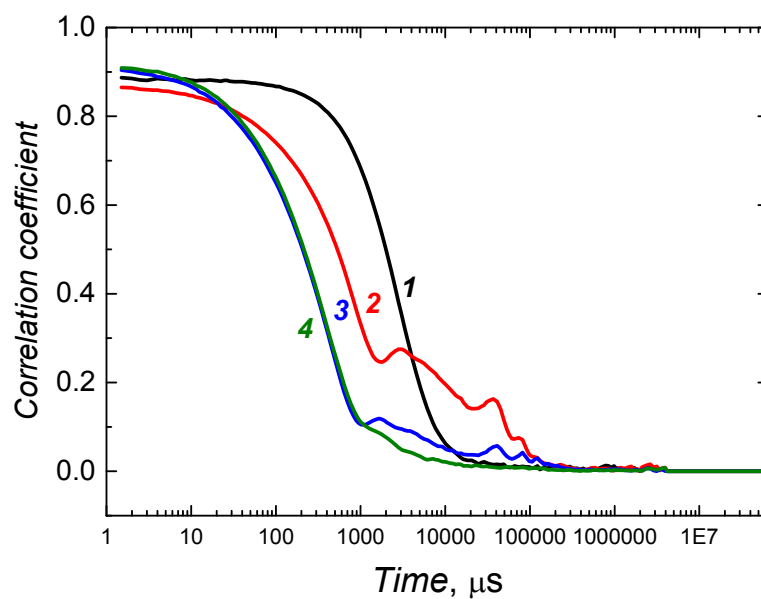


**Figure S5.** The correlation function intensity for **NIPAM-MA-BIS** nanogel particles in suspensions of pH of (1) 4.0, (2) 6.0, (3) 7.0, and (4) 8.0. The **NIPAM-MA-BIS** gel prepared by electrochemically initiated copolymerization of the **NIPAM**, **MA**, and **BIS** monomers of respective 20, 20, and 10 mM concentrations.

#### S4. MTT assay for IC<sub>50</sub> value

The cell solution after the passage was diluted to an approximate number of ~10 000 cells/well (controlled with Countess II Cell Counter) and seeded into a 96-well plate (Greiner Bio-One). Then, cells were incubated for 24 h at 37 °C to enable cell attachment. The medium was removed, and **NIPAM-MA-BIS** gels were added to the fresh culture medium at different concentrations (1000 µg/mL to 2 µg/mL). We performed five repeats for each concentration. Moreover, controls were repeated five times: blank - medium without cells, positive control - cells not treated with the tested particles, and negative control - dead cells, toxicant - 1%, v/v, Triton-X 100 (Sigma-Aldrich). The plate was incubated at 37 °C for 24 hours. Afterward, the medium was replaced with a culture medium containing 1 mM 3-(4,5-dimethylthiazol-2-yl)-2,5-diphenyltetrazolium bromide (MTT reagent, Thermo Fischer Scientific). We incubated cells for 4 h at 37 °C. Then, solutions were replaced with DMSO and incubated for 10 min. The absorbance in each well was measured at 540 nm wavelength using a Synergy HTX multi-mode reader (BioTek). Two independent cytotoxicity assays were performed.

##### *Data analysis*

The percentage of viable cells in each sample compared to the control was calculated from the absorbance measurement data using Equation S3:

$$\text{Viability [\%]} = \frac{\text{Measured value} \cdot \text{Average}_{\text{negative control}}}{\text{Average}_{\text{positive control}} \cdot \text{Average}_{\text{negative control}}} \quad (\text{S3})$$

Each data point averages five independent wells, and error bars correspond to the standard deviations. The IC<sub>50</sub> concentration was determined from a plot of cell viability as a function of nanoparticle concentration. Cell viability data were fitted with a Logistic Dose-Response model, with four fitting parameters (Equation S4)

$$y = \frac{A_1 - A_2}{1 + (x/IC_{50})^p} + A_2 \quad (\text{S4})$$

where A1 and A2 were upper and lower asymptotes, respectively; the IC<sub>50</sub> values were fitting parameters of the model. The fitting results are presented in Figures S6 and S7. The results obtained enabled determining the IC<sub>50</sub> value as 485 µg/mL. The dose-response graph is shown in Figure S6 in Supporting Information. The IC<sub>50</sub> value corresponds to 15-fold coverage of the growth surface (Figure S7 in Supporting Information). A significant decrease in cell viability

was observed for the highest concentrations (33% of living cells for 1 000  $\mu\text{g/ml}$ ). However, it is essential to remember that the  $\text{IC}_{50}$  value is closely related to the nanoparticles' coverage of the surface area available for cell growth.

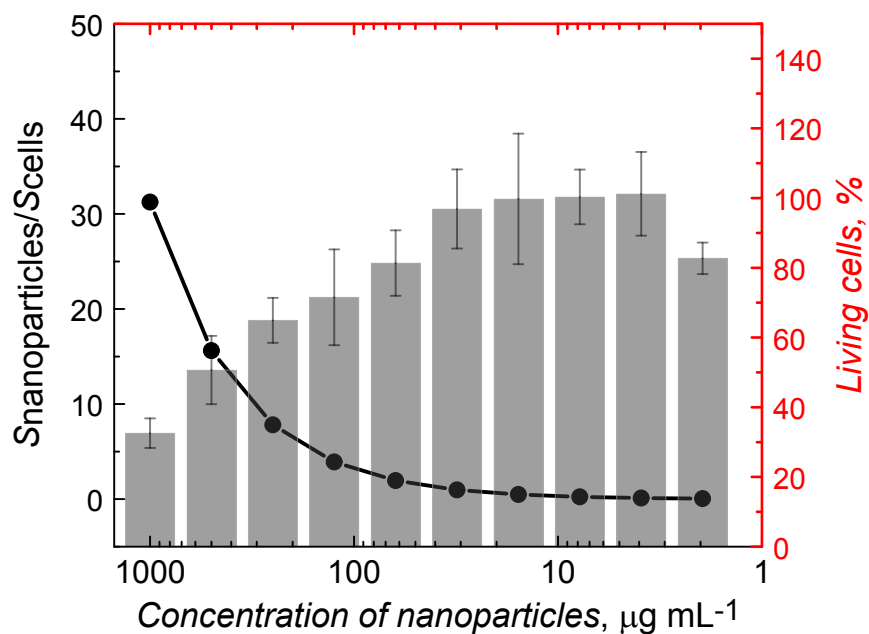


**Figure S6.** HeLa cells viability as a function of nanoparticles' concentration. The black curve shows the ratio of the surface area occupied by nanoparticles to the surface area available to cells ( $S_{\text{nanoparticles}}/S_{\text{cells}}$ ).

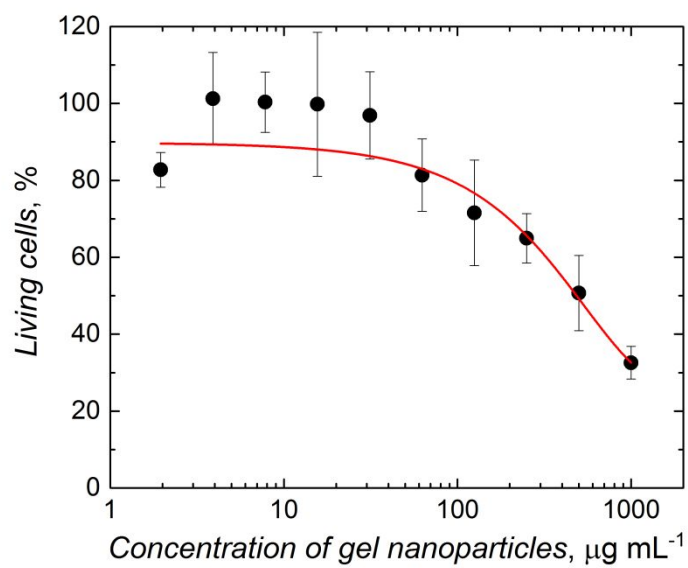


**Figure S7.** Viability of HeLa cells incubated for 24 h with **NIPAM-MA-BIS** gel nanoparticles as a function of gel nanoparticles' concentration, with the  $\text{IC}_{50}$  value ( $485 \mu\text{g mL}^{-1}$ ) based on MTT assay.

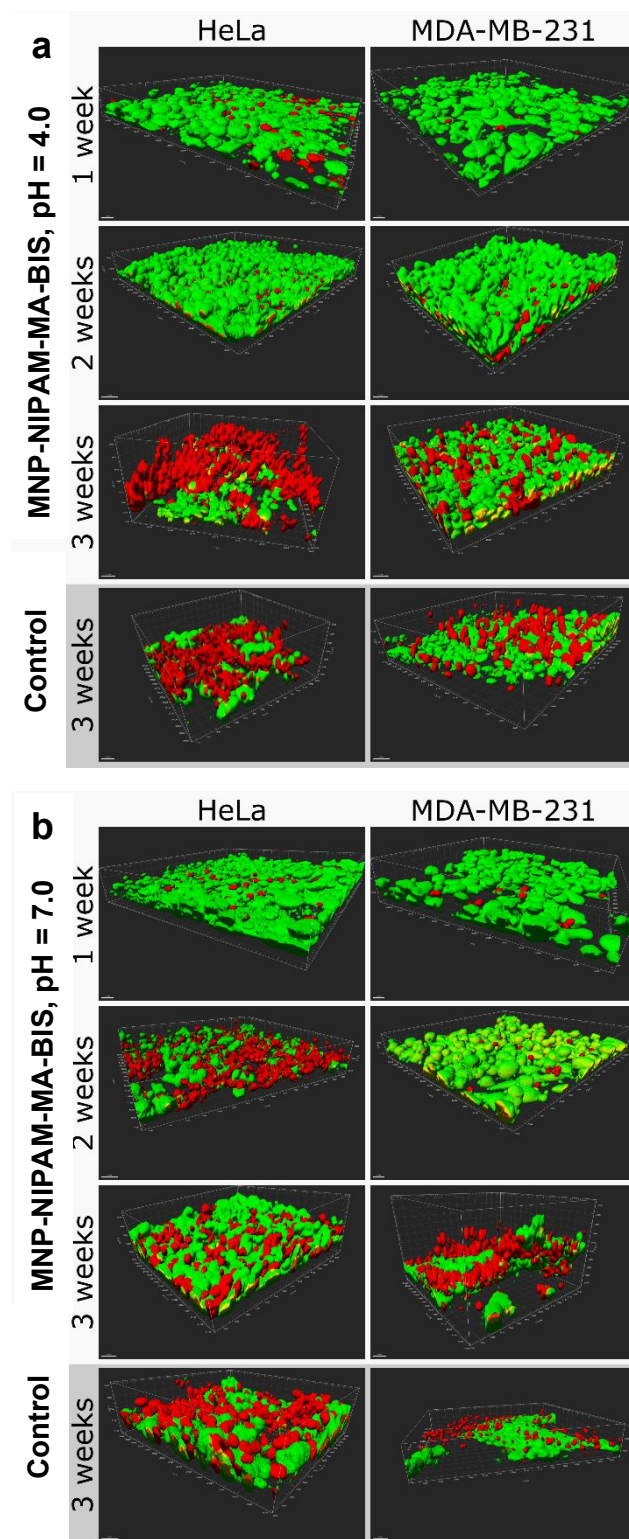


**Figure S8.** Confocal microscopy images of the long-term three-dimensional tissue culture on **MNP-NIPAM-MA-BIS** core-shell particles. Gel particles dispersed in solutions of pH of (a) 4.0 and (b) 7.0. Green objects are viable cells stained with calcein-AM, and red objects are nuclei of dead cells stained with propidium iodide. Scale horizontal bars correspond to 30  $\mu\text{m}$ .

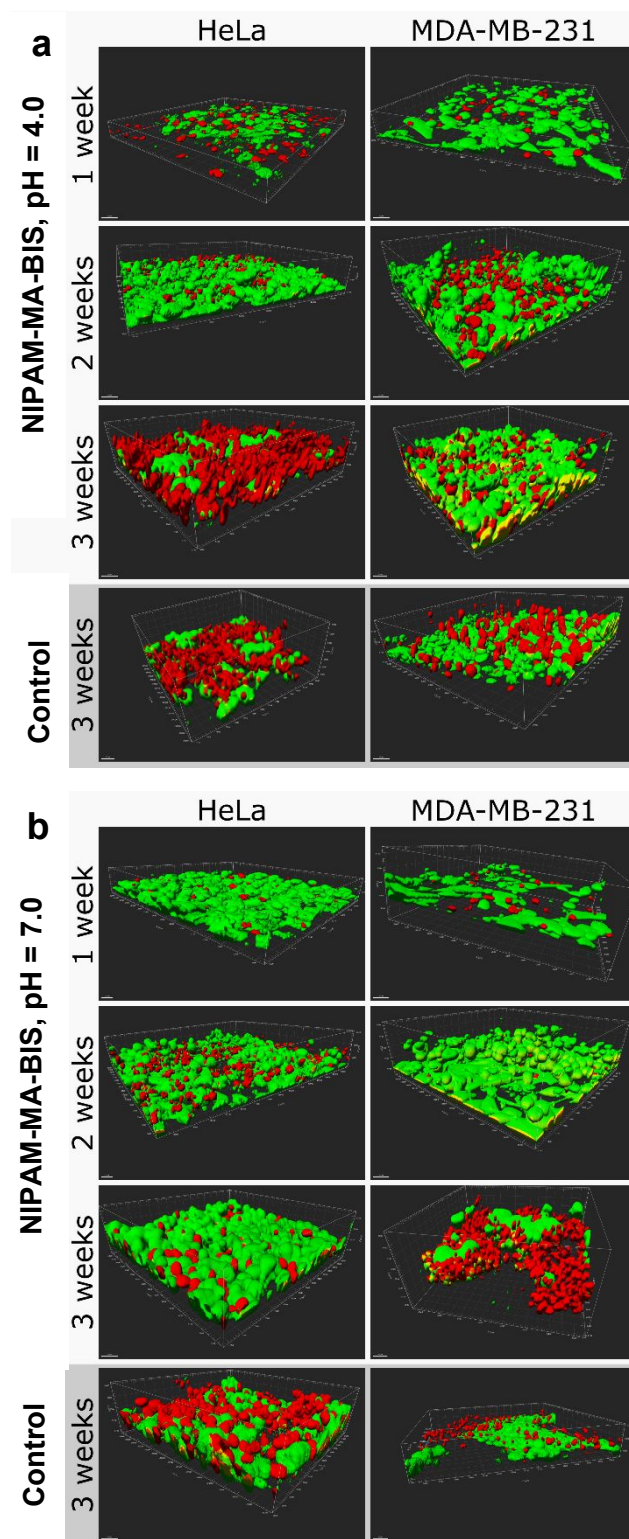


**Figure S9.** Confocal microscopy images of the long-term three-dimensional tissue culture on NIPAM-MA-BIS core-shell particles. Microgel particles dispersed in solutions of pH of (a) 4.0 and (b) 7.0. Green objects are viable cells stained with calcein-AM, and red objects are nuclei of dead cells stained with propidium iodide. Scale horizontal bars correspond to 30  $\mu\text{m}$ .

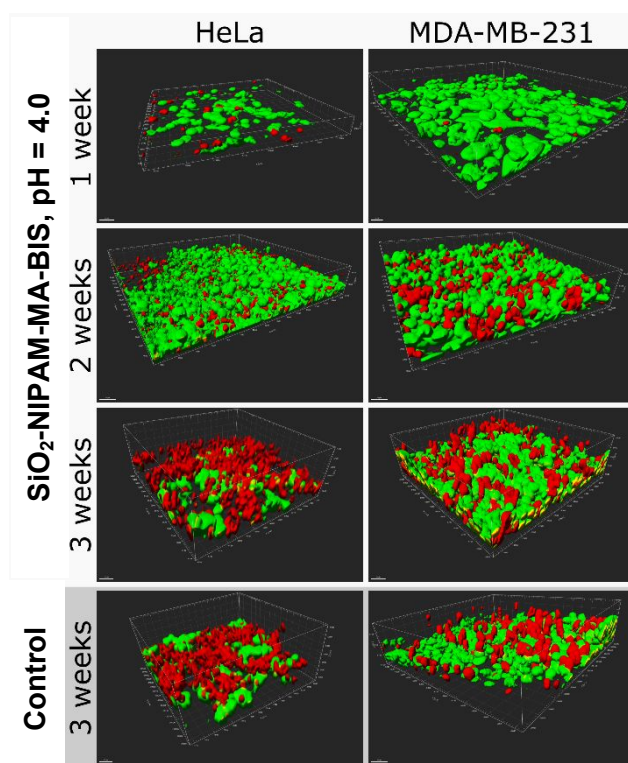


**Figure S10.** Confocal microscopy images of the long-term three-dimensional tissue culture on SiO<sub>2</sub>-NIPAM-MA-BIS core-shell particles. Gel particles were dispersed in solutions of pH of (a) 4.0 and (b) 7.0. Green objects are viable cells stained with calcein-AM, and red objects are nuclei of dead cells stained with propidium iodide. Scale horizontal bars correspond to 30 μm.

## REFERENCES

- (1) Yasmeen, N.; Kalecki, J.; Borowicz, P.; Kutner, W.; Sharma, P. S. Electrochemically Initiated Synthesis of Polyacrylamide Microgels and Core-shell Particles. *ACS Appl. Polym. Mater.* **2022**, *4*, 452-462.
- (2) Kaniewska, K.; Karbarz, M.; Stojek, Z. Electrochemical Attachment of Thermo- and pH Sensitive Interpenetrating-Polymers-Network Hydrogel to Conducting Surface. *Electrochim. Acta* **2015**, *179*, 372-378.